

Supporting information

Genesis of a highly active Cerium Oxide-Supported Gold Catalyst for CO Oxidation

Veronica Aguilar-Guerrero and Bruce C. Gates*

Experimental

A. *Sample preparation*

Samples were synthesized and handled in the absence of moisture and air by using a double manifold Schlenk vacuum line and a dry box purged with Ar that was recirculated through traps containing of supported Cu and zeolites 4A for removal of O₂ and moisture. The sample containing 1 wt% Au on CeO₂ was synthesized from Au(CH₃)₂(C₅H₇O₂) (Strem 99.9%) and high-surface-area CeO₂ (Daiichi, 99.9%, 173.3 m²/g and average particle size 45.7 nm, with this information provided by the supplier).

The catalyst was prepared by forming a slurry of Au(CH₃)₂(C₅H₇O₂) in *n*-pentane with CeO₂ powder that had been partially dehydroxylated under vacuum at 673 K. The slurry was stirred for 24 h, and the solvent was removed by evacuation for 24 h.

B. *X-Ray Absorption Spectroscopy (XAS)*

Data characterizing the as-prepared and treated samples were recorded at 298 K. Approximately 0.2 g of sample was used for this purpose.

The XAS experiments were performed at beam line 2-3 of the Stanford Synchrotron radiation Laboratory (SSRL) at the Stanford Linear Accelerator Center, Stanford, CA, and at beam line X-18B of the National Synchrotron Light Source (NSLS) at Brookhaven National Laboratory, Upton, NY. The

storage ring electron energy was 3 GeV at SSRL and 2.7 GeV at BNL; the current varied in the range of 50–100 mA at SSRL and 140–240 mA at NSLS.

The spectra were collected in fluorescence mode, which was chosen rather than transmission because of the high absorbance of Ce at the Au L_{III} edge (11919 eV). Higher harmonics in the X-Ray beam were minimized by detuning the Si(III) double crystal monochromator by 20–25% at the Au L_{III} edge. The Ge detector with 13 channels allowed recording of 13 signals per scan, and each reported spectrum is an average of at least four scans. The resolution of the monochromator was 0.5 eV.

The software XDAP¹ was used to analyze the EXAFS data with a difference file technique. The functional that was minimized and the function used to model are given elsewhere.¹

Data analysis was carried out with unfiltered data; the k range is indicated in Table SI1 (k is the wave vector), and the r range was 1 to 5 Å (r is the absorber (Au)—backscatterer distance). The candidate models included Au–Au, Au–O, Au–C, and Au–Ce contributions. Iterative fitting was done in r space by using k^1 -, k^2 -, and k^3 - weightings until optimum agreement was obtained between the data and the fits with all the applied k -weightings considered. The statistically justified number of free parameters in the analysis of the EXAFS data of the various samples was estimated on the basis of the Nyquist theorem² to be approximately 12 to 20 (Table SI1); 8–12 parameters were used in the fits depending on the number of contributions that were found in the data analysis. No satisfactory fit was found with any model including Au–Ce contributions.

The models providing the best fits for each sample are stated in the text of the paper. The EXAFS parameters determined in the best-fitting model for each sample are summarized in the paper, and additional details are given in Table SI2.

In the data fitting for the as-prepared sample and that after use as a catalyst for 2 h onstream in the flow reactor, both Au–O and Au–C contributions were found—at distances close to each other, that is, 2.09 and 2.05 Å, respectively, for the former sample and 2.09 and 2.13 Å, respectively, for the latter. Although these distances are close to each other and low- Z scatterers are sometimes difficult to distinguish from each other with EXAFS spectroscopy, an exchange of these contributions did not lead to

Supplementary Material (ESI) for Chemical Communications

This journal is (c) The Royal Society of Chemistry 2007

a satisfactory fit, as indicated by an increase in the value of the goodness of fit when the switch was made. Thus, we are confident that the contributions were distinguishable in our case.

Table SII. EXAFS results: goodness of fit parameter and variance between data and fit obtained upon addition of each contribution used in the analysis

<i>Sample/conditions of scan</i>	<i>shell</i>	ϵ_v^2 ^a	k^n -weighted variance (%) ^{b,c}	k^l -weighted variance (%) ^b	k -range (\AA^{-1})	χ^2
As-prepared catalyst/298 K under He flow at 100 mL (min) ⁻¹	Au–Au	-	-	-	2.99–12.4	29.6
	Au–O	61	57	42		
	Au–C	5.9	5.6	6.7		
After 2 h of CO oxidation catalysis at 353 K/353 K during catalysis	Au–Au	-	-	-	2.94–12.4	4.1
	Au–O	21	56	65		
	Au–C	2.9	5.7	11		
After 24 h of CO oxidation catalysis at 353 K/298 K under N ₂ after catalysis	Au–Au	28	70	49	2.69–12.2	7.6
	Au–O	5.0	59	15		
After 48 h of CO oxidation catalysis at 353 K/298 K under N ₂ after catalysis	Au–Au	5.8	29	12	2.99–13.1	36.8

Goodness of fit parameter; the meaning of these values is as follows: (a) when only one contribution was included, it was generally characterized by a larger value of ϵ_v^2 than when two contributions were included; this means that the goodness of the fit improved upon addition of another shell. For example, in the first entry in the table, when only an Au–O contribution was included, the value of ϵ_v^2 was 61, and when an Au–C contribution was included with this in the fit, the value of ϵ_v^2 decreased to 5.9, indicating a substantially better fit and the validity of including both contributions in the fit. ^bVariance between the k -weighted Fourier transform of the raw data and the fit over the fitting range (1–4 \AA); the stated values are the variance obtained first with only the one contribution shown and, second (giving the smaller value of the variance), after addition of the second contribution to the fit. In the calculation representing the as-prepared sample and the sample that had been used for 2 h as a CO oxidation catalyst, the calculation was done for n (the weighting of k in the Fourier transformation) = 0 (because there were no Au–Au contributions); on the other hand, for samples characterized after 24 and 48 h of catalytic reaction, the value of n was 3, because there were significant Au–Au contributions.

Table SI2. EXAFS parameters characterizing the samples treated at various stages during CO oxidation catalysis^a

<i>Sample/conditions of scan</i>	shell	<i>N</i>	<i>R</i> (Å)	$10^3 \times \Delta\sigma^2$ (Å ²)	ΔE_0 (eV)
As-prepared catalyst/298 K under He flow at 100 mL (min) ⁻¹	Au–Au	b	b	b	b
	Au–O	2.0 (0.1)	2.09 (0.00)	5.6 (0.9)	-6.9 (0.3)
	Au–C	2.1 (0.1)	2.05 (0.00)	11.0 (1.0)	-12.3 (0.4)
After 2 h of CO oxidation catalysis at 353 K/353 K during catalysis	Au–Au	b	b	b	b
	Au–O	2.2 (0.1)	2.09 (0.01)	-0.1 (0.7)	-6.8 (0.4)
	Au–C	2.0 (0.0)	2.13 (0.00)	7.3 (0.4)	-11.9 (0.3)
After 24 h of CO oxidation catalysis at 353 K/298 K under N ₂ after catalysis	Au–Au	4.0 (0.1)	2.82 (0.01)	11.3 (0.3)	-5.8 (0.1)
	Au–O	0.7 (0.0)	2.08 (0.02)	1.6 (0.2)	2.2 (0.2)
After 48 h of CO oxidation catalysis at 353 K/298 K under N ₂ after catalysis	Au–Au	5.9 (0.1)	2.79 (0.02)	10 (1.6)	0.42 (0.01)

^a Notation: *N* = coordination number; *R* = distance between absorber and backscatterer atoms; $\Delta\sigma^2$ = Debye-Waller factor relative to reference; ΔE_0 = inner potential correction. Numbers in parentheses are the calculated errors and represent precisions, not accuracies. Estimated accuracies are as follows: Au–Au, *N* ± 20%, *R* ± 0.02 Å, $\Delta\sigma^2$ ± 20%, ΔE_0 ± 20%; Au–O, *N* ± 10%, *R* ± 0.02 Å, $\Delta\sigma^2$ ± 20%, ΔE_0 ± 20%; Au–C, *N* ± 10%, *R* ± 0.03 Å, $\Delta\sigma^2$ ± 20%, ΔE_0 ± 20%.

EXAFS data characterizing gold foil and parameters representing the structure of bulk gold were used as references for the phase shifts and backscattering amplitudes of the Au–Au interaction, respectively. Na₂Pt(OH)₆ was used as a reference for the Au–O_{support} reference file. Au(CH₃)₂(C₅H₇O₂) mixed with BN was used as a reference for the Au–C contribution.

XANES spectra of the samples were compared with those of compounds of gold in various oxidation states. Figure SI1 shows the XANES spectra compounds incorporating Au^{III}, Au^I, and Au⁰, measured at room temperature.

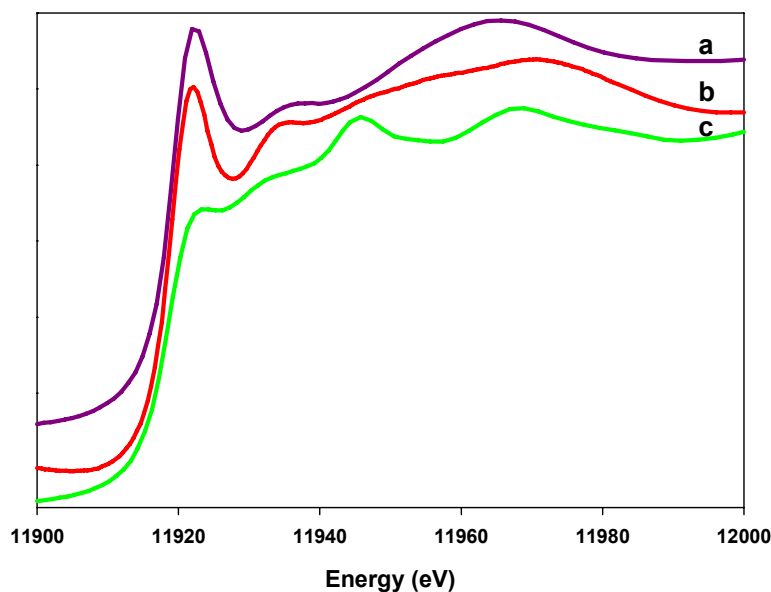


Figure S11. XANES spectra of reference gold compounds: (a) $\text{Au}(\text{CH}_3)_2(\text{acac})$, (b) AuCl , and (c) Au foil.

C. Mass Spectrometry

Effluent gases from the reactor were characterized with an on-line Omni StarTM Pfeiffer Vacuum mass spectrometer running in multi-ion monitoring mode. The main fragments recorded were as follows: H_2 ($m/e = 2$), CH_4 ($m/e = 12, 13, 14, 15,$ and 16), H_2O ($m/e = 16, 17,$ and 18), CO ($m/e = 12, 14, 16,$ and 28), O_2 ($m/e = 16$ and 32), and CO_2 ($m/e = 16, 28, 30,$ and 44). All signals are reported relative to that of the He carrier gas ($m/e = 4$) to remove effects of pressure fluctuations. Products were analyzed by mass spectrometry, and some results are shown in Figure S117. Signals corresponding to CO and O_2 decreased with time as the signal corresponding to CO_2 increased, demonstrating conversion of CO into CO_2 as the reaction took place.

D. CO Oxidation Catalysis

CO oxidation catalysis was carried at various temperatures and atmospheric pressure in a standard once-through, nearly isothermal tubular packed-bed flow reactor. The catalyst mass was 0.025 g, and the catalyst powder was mixed with particles of inert, non-porous $\alpha\text{-Al}_2\text{O}_3$ and then introduced into the reactor in a glove box and transferred to a flow system without coming in contact with air or moisture.

Supplementary Material (ESI) for Chemical Communications

This journal is (c) The Royal Society of Chemistry 2007

The total flow rate was 100 mL/min. The experiment was carried out at atmospheric pressure, and the partial pressures of CO and O₂ were equal to 10.1 and 5.7 mbar, respectively, and the balance was He. Conversions were determined by chromatographic analysis of the product stream; they were determined on the basis of CO and O₂ consumptions. CO₂ was the only observed product. An on-line gas chromatograph (Hewlett-Packard, HP-5890 Series II) (with a thermal conductivity detector) was used to separate any water that might have been present from other product gases in a polar column (Hayesep Q, 8' x 1/8", 80–100 mesh), followed by separation of O₂, and CO in a zeolite 5A column (Chrompack, PLOT fused silica, 25-m x 0.53 mm).

Calcined ceria at 673 K was used in blank experiments at both 298 and 353 K (the ceria was used instead of catalyst in these experiments), and the CO conversion was found to be negligible in both cases.

Table S13. Comparison of conditions used by various authors for testing the performance of supported gold catalysts for CO oxidation at 1 bar

Catalyst	Feed composition (Partial pressure P , mbar); total flow rate/mass of catalyst, mL/min \times g)	CO Conversion (%)	Au content of catalyst (wt %)
Au/CeO ₂ * (initially)	$P_{\text{CO}} = 10.1, P_{\text{O}_2} = 5.7$ $P_{\text{He}} = 983;$ 4000	1.3	1.0
Au/CeO ₂ * (after activation, Figure 2 in paper)	same as above	increasing beyond approximately 90% when experiment stopped	1.0
Au/CeO ₂ * (activated, Figure 3 in paper)	same as above	30 to 50	1.0
Au/La ₂ O ₃ ³	$P_{\text{CO}} = 15.6, P_{\text{O}_2} = 15.6$ $P_{\text{He}} = 982;$ 500	3 to 10	1.0
Au/CeO ₂ ⁴	$P_{\text{CO}} = 2.0, P_{\text{O}_2} = 200.6$ $P_{\text{He}} = 810.6;$ 2050	1.8	2.8
Au/zeolite NaY ⁵	$P_{\text{CO}} = 15.6, P_{\text{O}_2} = 15.6$ $P_{\text{He}} = 982;$ 333	40 to 5	1.0
Au/Al ₂ O ₃ ⁶	$P_{\text{CO}} = 15.6, P_{\text{O}_2} = 15.6,$ $P_{\text{He}} = 982;$ 5000	44 to 6	1.1
Au/Fe ₂ O ₃ ⁷	$P_{\text{CO}} = 9.1, P_{\text{O}_2} = 921,$ $P_{\text{He}} = 91.1;$ 1100	100	2.1
Au/Fe ₂ O ₃ ⁸	$P_{\text{CO}} = 9, P_{\text{O}_2} = 921, P_{\text{He}}$ $= 91.1;$ 1100	65 to 100	5.0
Au/TiO ₂ ⁹	$P_{\text{CO}} = 10.1, P_{\text{O}_2} = 211,$ $P_{\text{N}_2} = 783, P_{\text{other}} = 10.1;$ 1100	<10	0.7

*This work

Data Analysis

EXAFS Spectroscopy

Estimated errors in EXAFS parameters are as follows:

Au–low-*Z* scatterers: error in *N*: $\pm 10\%$, in *R*: $\pm 0.02 \text{ \AA}$. Au–high-*Z* scatterers: error in *N*: $\pm 20\%$;
error in *R*: $\pm 0.02 \text{ \AA}$.

Catalytic reaction experiments

Specifics regarding calculations of turnover frequency, TOF:

In the experiment with the sample during the apparent steady state, the CO conversion was about 1.3%. This near steady state lasted approximately 2 h. The TOF values were calculated by taking into account the total amount of Au that was present in the sample, assuming that it was all exposed; thus, the turnover frequency is considered to be a lower limit of the actual value and a good approximation because the clusters are so small that almost all the Au atoms were surface atoms. Our calculations ignore the possible lack of accessibility of gold atoms at the metal–support interface.

The literature is lacking in well-defined values of turnover frequency for comparison with ours, and the data included here for comparison are nearly complete for catalysis of CO oxidation at temperatures in the range that we used.

Turnover frequencies for the catalysts compared with ours were calculated in various ways, as reported by the respective authors. For example, Haruta⁹ et al. calculated the number of Au surface atoms from the Au particle size assuming a cubic structure. The literature is lacking in well-defined valued of turnover frequency for comparison with ours, and the data included here are nearly complete for catalysis of CO oxidation at temperatures in the range that we used.

The data are compared with the best fits in the following figures. The difference-file plots indicate the fits to the individual contributions.

A) AS-PREPARED SAMPLE

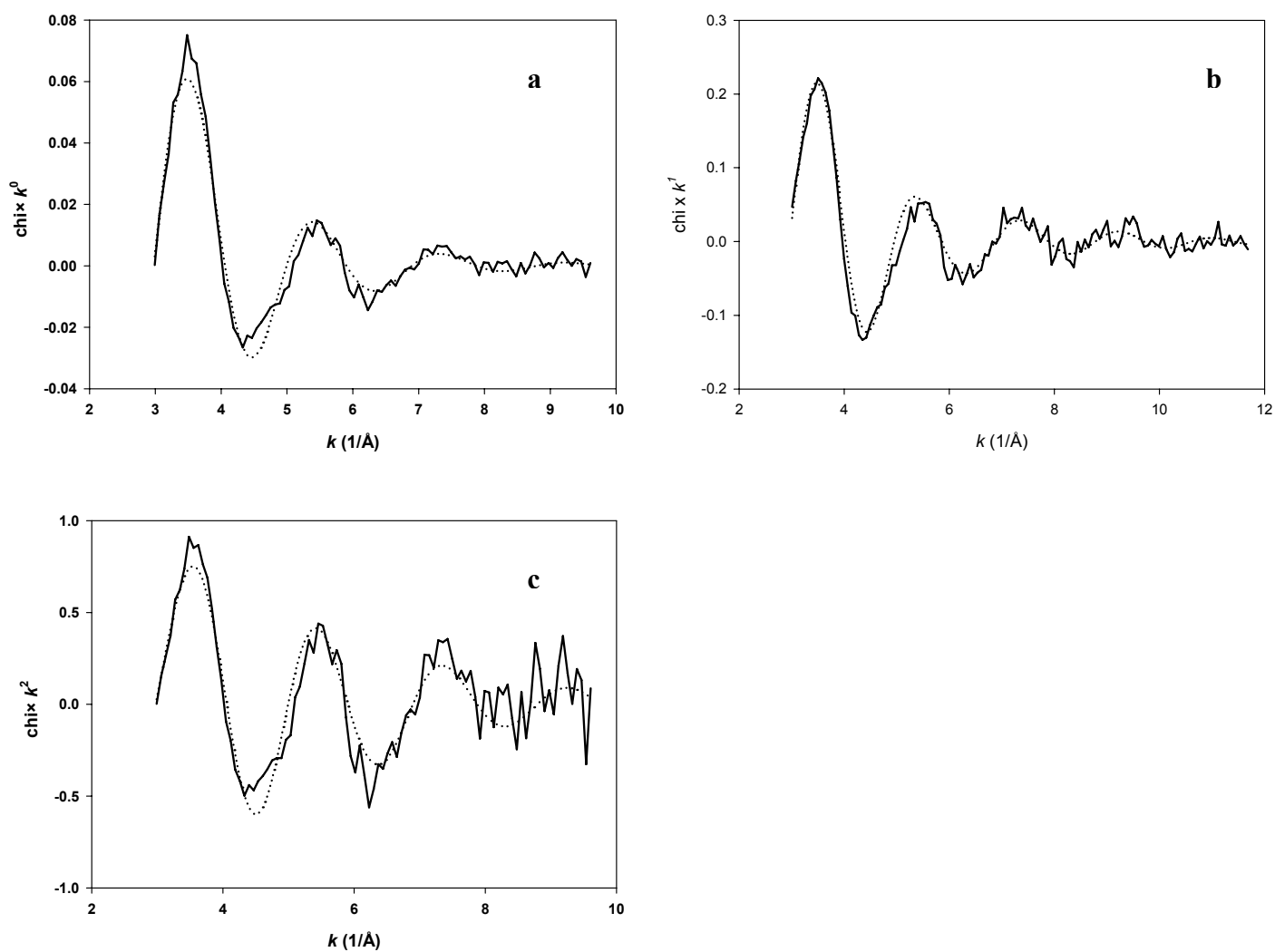


Fig. SI2. EXAFS function characterizing the as-prepared sample scanned at 298 K (a) k^0 -weighted, (b) k^1 -weighted, and (c) k^2 -weighted. The solid line represents the experimental results. The dotted line represents the sum of the calculated contributions with the best-fit model.

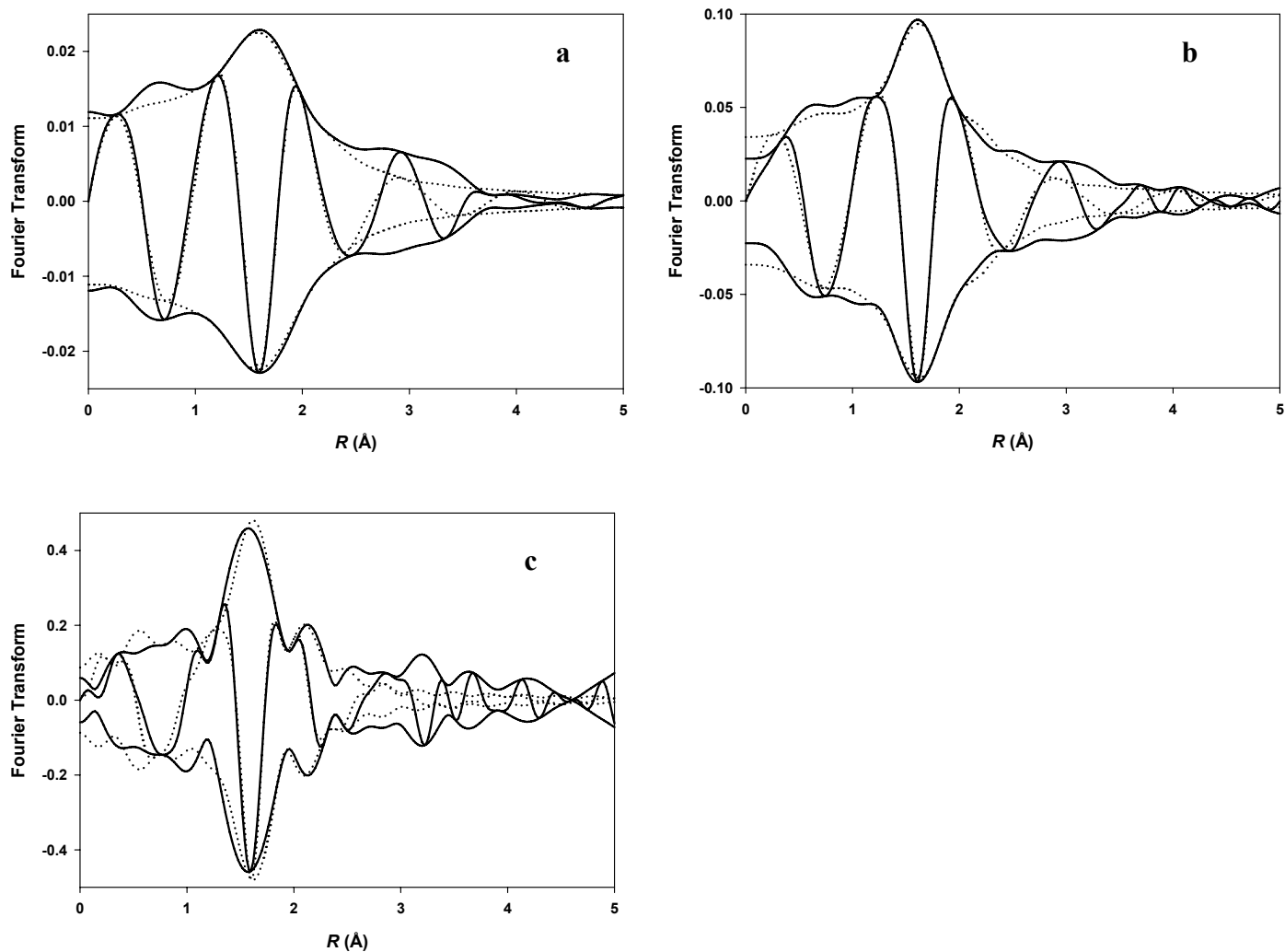


Fig. S13. Imaginary part and magnitude of uncorrected Fourier transform of experimental EXAFS function (solid line) and sum of the calculated contributions (dotted line) characterizing the as-prepared sample at 298 K. (a) k^0 -weighted, (b) k^1 -weighted, and (c) k^2 -weighted.

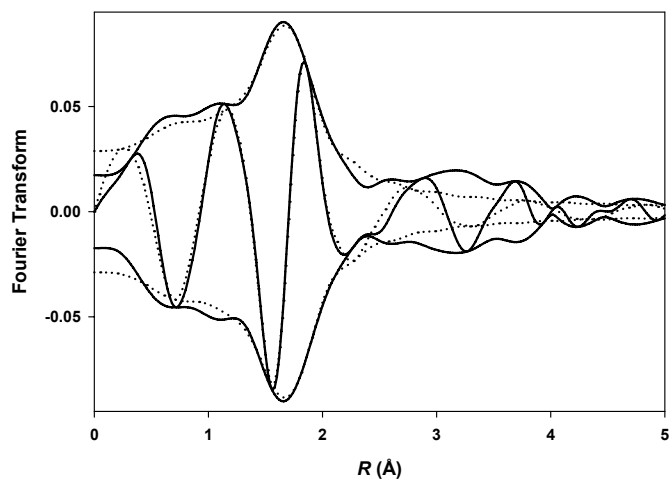


Fig. SI4. Residual spectrum illustrating the individual EXAFS Au–O contribution characterizing the as-prepared sample at 298 K. Imaginary part and the magnitude of the Fourier transform (k^1 -weighted) of the raw data minus the calculated Au–C contribution (solid line); the calculated Au–O contribution is shown as the dotted line.

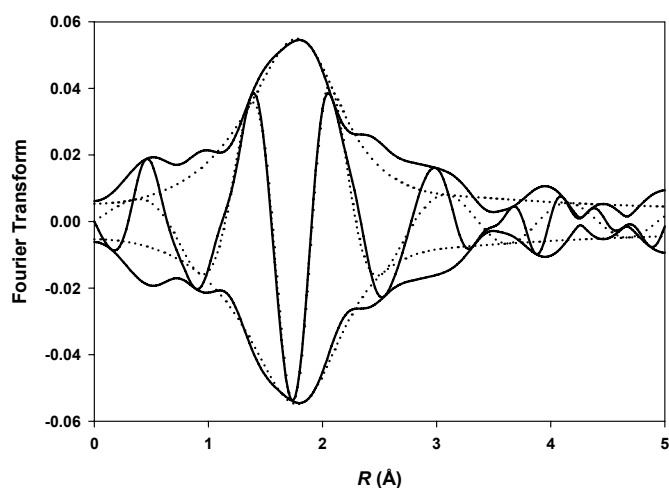
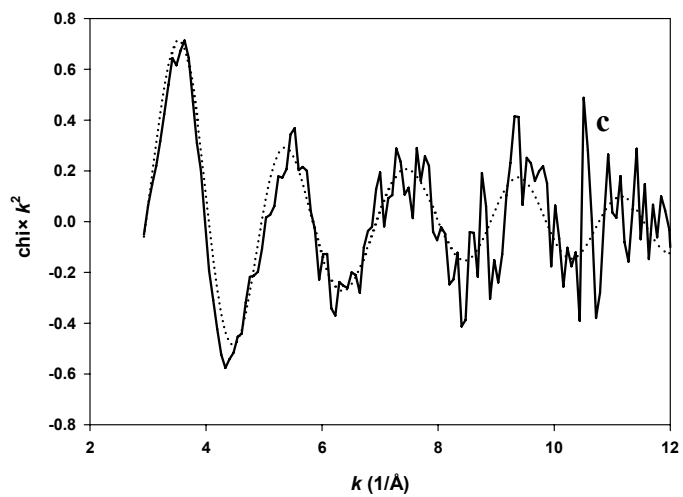
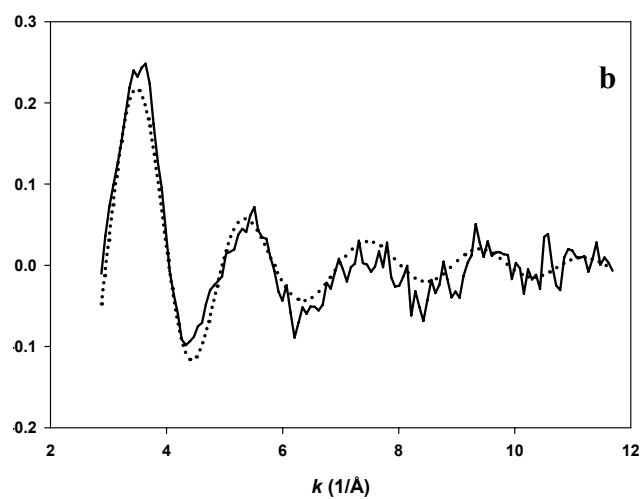
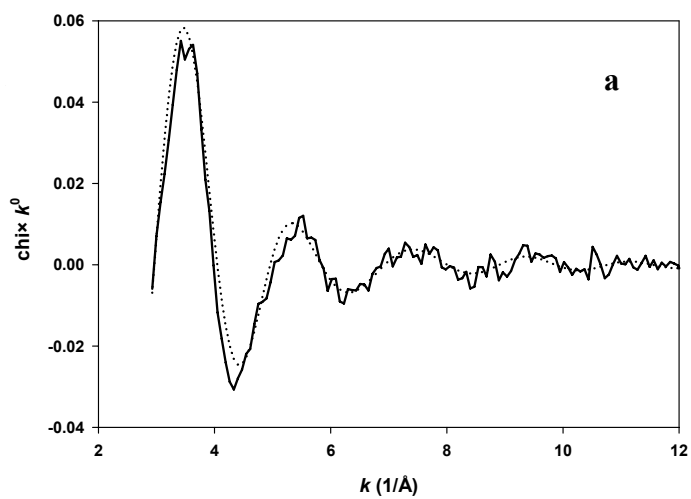


Fig. SI5. Residual spectrum illustrating the individual Au–C EXAFS contribution characterizing the as-prepared sample at 298 K. Imaginary part and magnitude of the Fourier transform (k^1 -weighted) of the raw data minus the fitted Au–O contribution, representing the Au–C contribution, shown as the solid line. The dotted line represents the calculated Au–C contribution.

B) APPARENT STEADY STATE AT 353 K DURING CO OXIDATION CATALYSIS



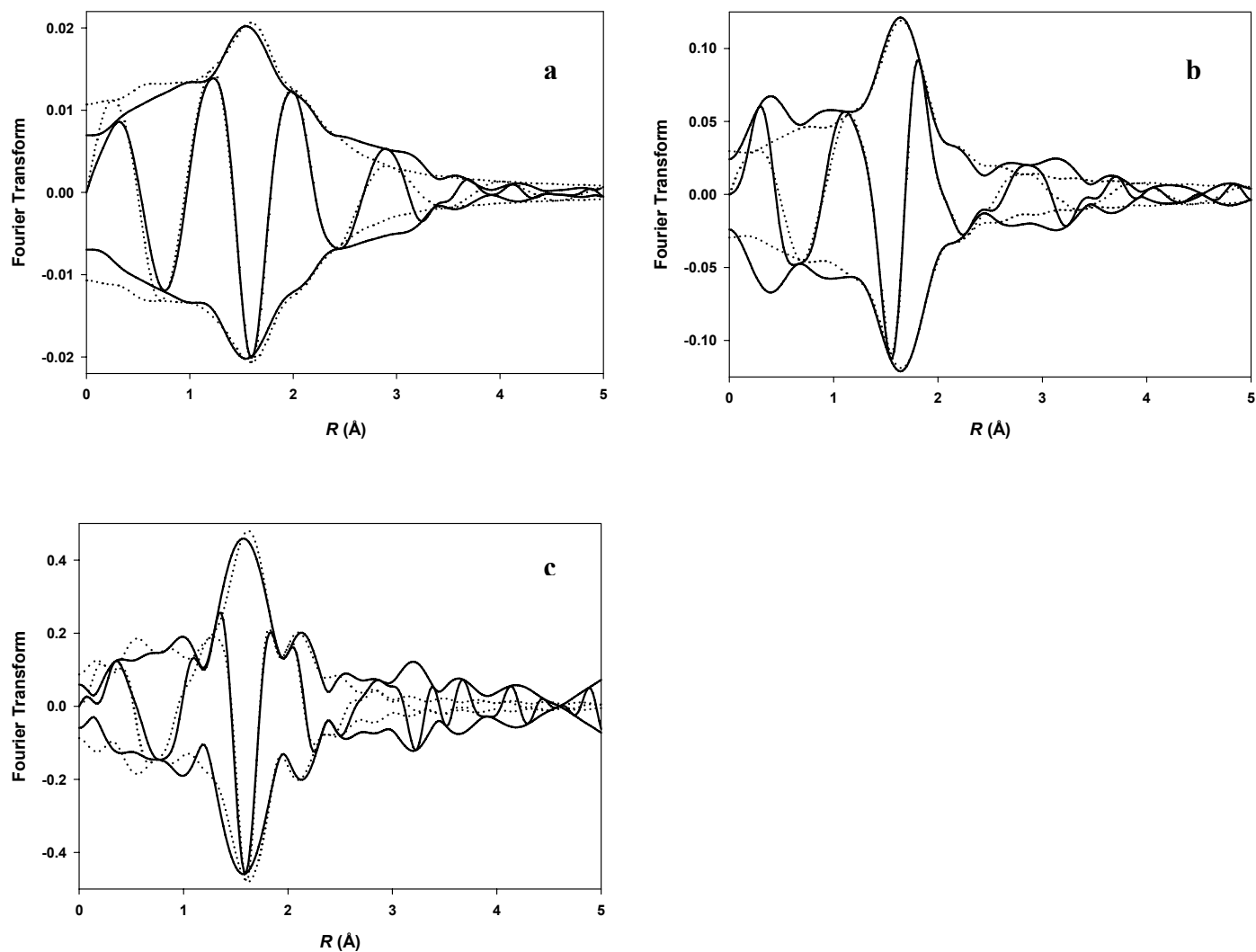


Fig. SI7. Imaginary part and magnitude of uncorrected Fourier transform of experimental EXAFS function (solid line) and sum of the calculated contributions (dotted line) characterizing the sample under CO oxidation reaction conditions at 353 K. (a) k^0 -weighted, (b) k^1 -weighted and, (c) k^2 -weighted.

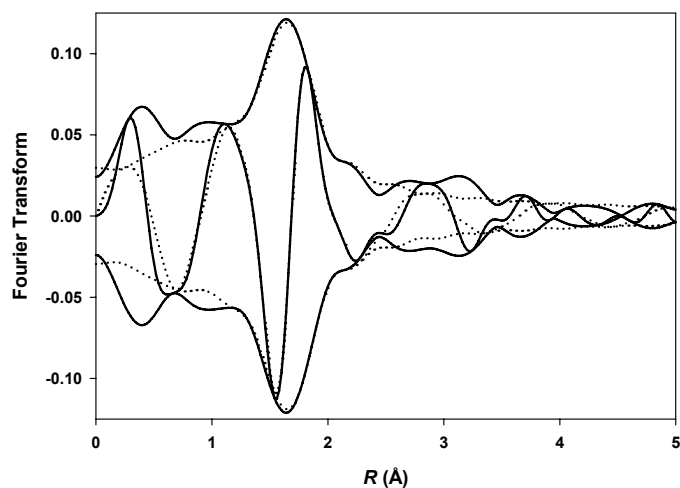


Fig. SI8. Residual spectra illustrating the individual EXAFS Au–O contribution in the spectrum of the sample under CO oxidation reaction conditions at 353 K. The solid lines represent the imaginary part and magnitude of the Fourier transform (k^1 -weighted) of the raw data minus the calculated Au–C contribution; the calculated Au–O contribution is shown as a dotted line.

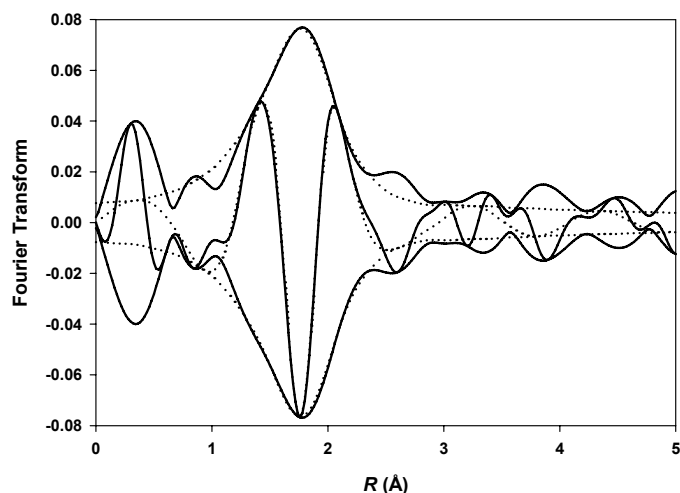


Fig. SI9. Residual spectra illustrating the individual EXAFS Au–C contribution in the spectrum of the sample under CO oxidation reaction conditions at 353 K. Imaginary part and the magnitude of the Fourier transform (k^1 -weighted) of the raw data minus the calculated Au–O contribution (solid line); the calculated Au–C contribution is shown as a dotted line.

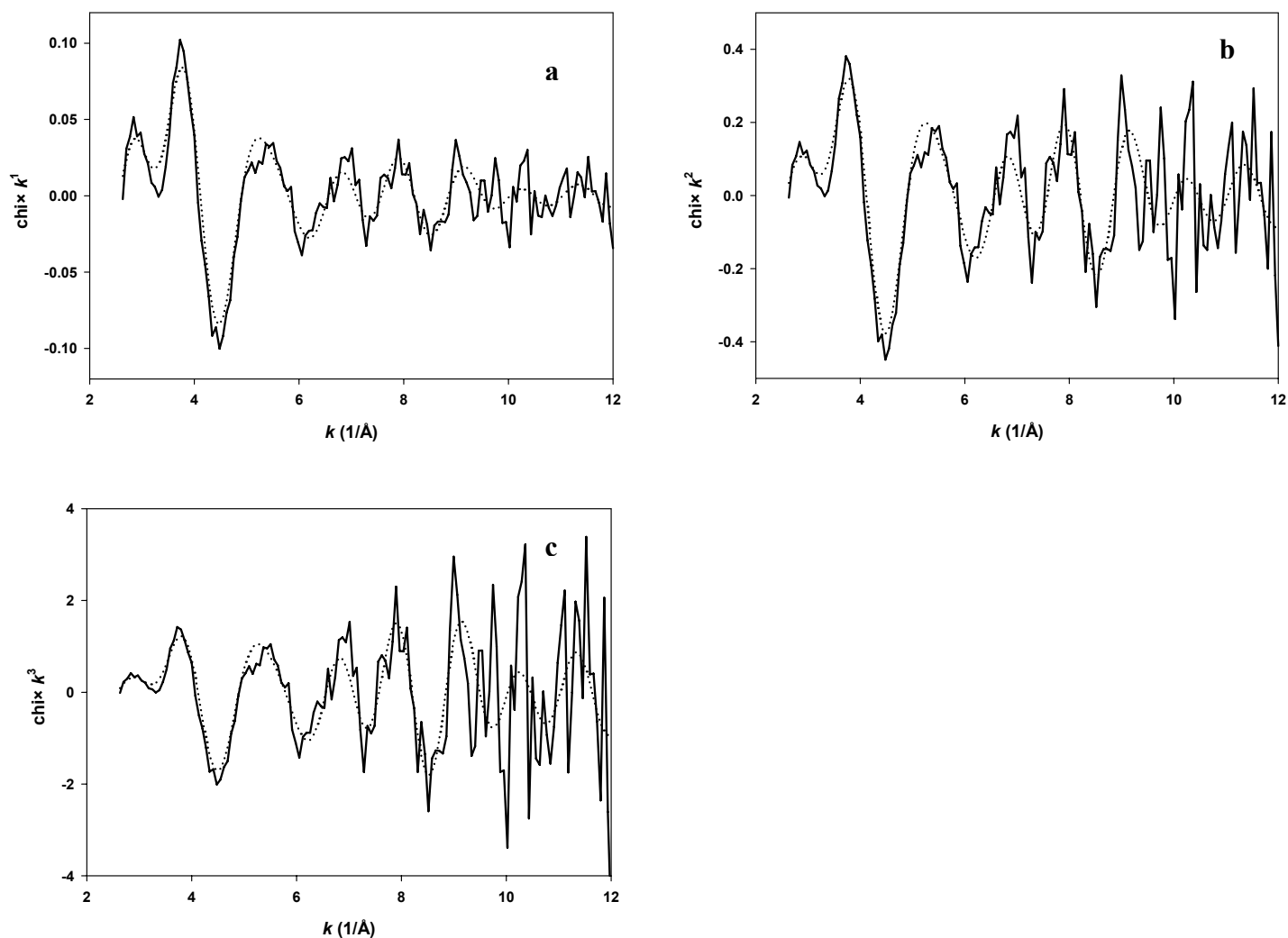


Fig. SI10. Experimental EXAFS function (solid line) and sum of the calculated contributions (dotted line) characterizing the sample after 24 h under CO oxidation reaction conditions at 353 K. (a) k^1 -weighted, (b) k^2 -weighted and, (c) k^3 -weighted. The k^3 -weighting of the data over emphasizes the deviations between the data and the fit at high values of k .

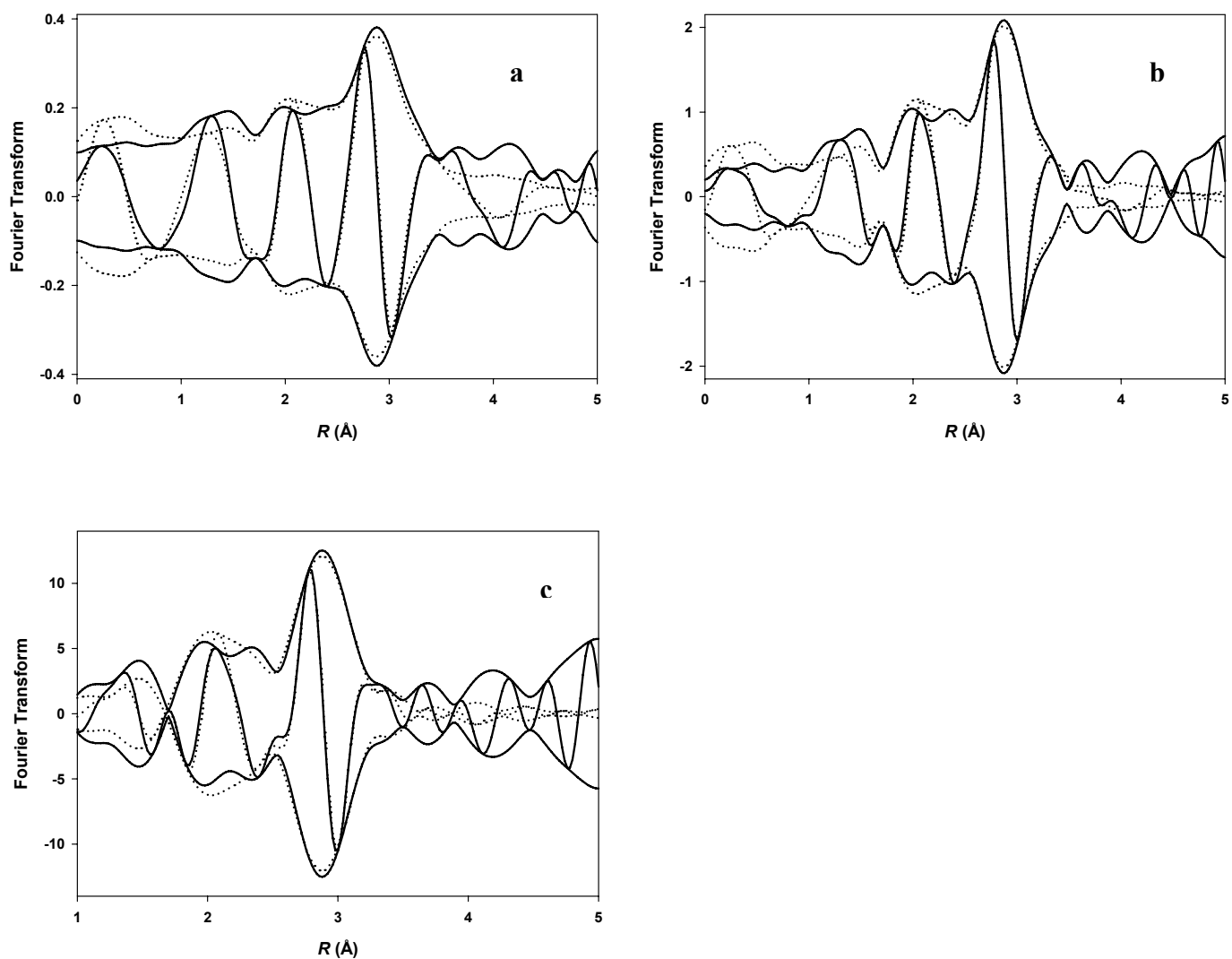


Fig. SI11. Imaginary part and magnitude of corrected Fourier transform of experimental EXAFS function (solid line) and sum of the calculated contributions (dotted line) characterizing the sample after 24 h under CO oxidation catalysis at 353 K. (a) k^1 -weighted, (b) k^2 -weighted and, (c) k^3 -weighted

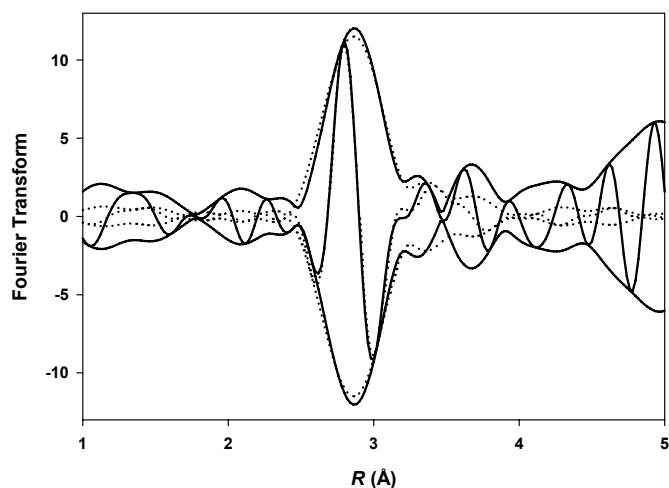


Fig. SI12. Residual spectrum illustrating the individual EXAFS Au–Au contribution in the spectrum of the sample under CO oxidation reaction conditions at 353 K. The solid lines represent the imaginary part and magnitude of the Fourier transform (k^3 -weighted) of the raw data minus the calculated Au–O contribution; calculated Au–Au contribution is shown as a dotted line.

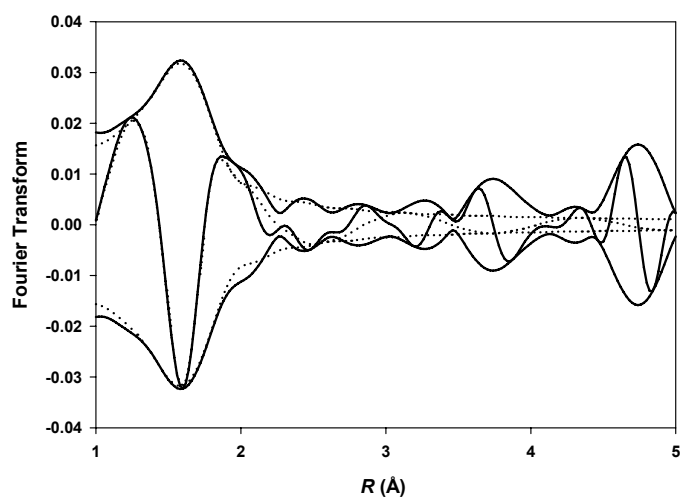


Fig. SI13. Residual spectrum illustrating the individual EXAFS Au–O contribution characterizing the sample under CO oxidation reaction conditions at 353 K. The solid lines represent the imaginary part and magnitude of the Fourier transform (k^1 -weighted) of the raw data minus the calculated Au–Au contribution (solid line) and the calculated Au–O contribution is thus shown (dashed line).

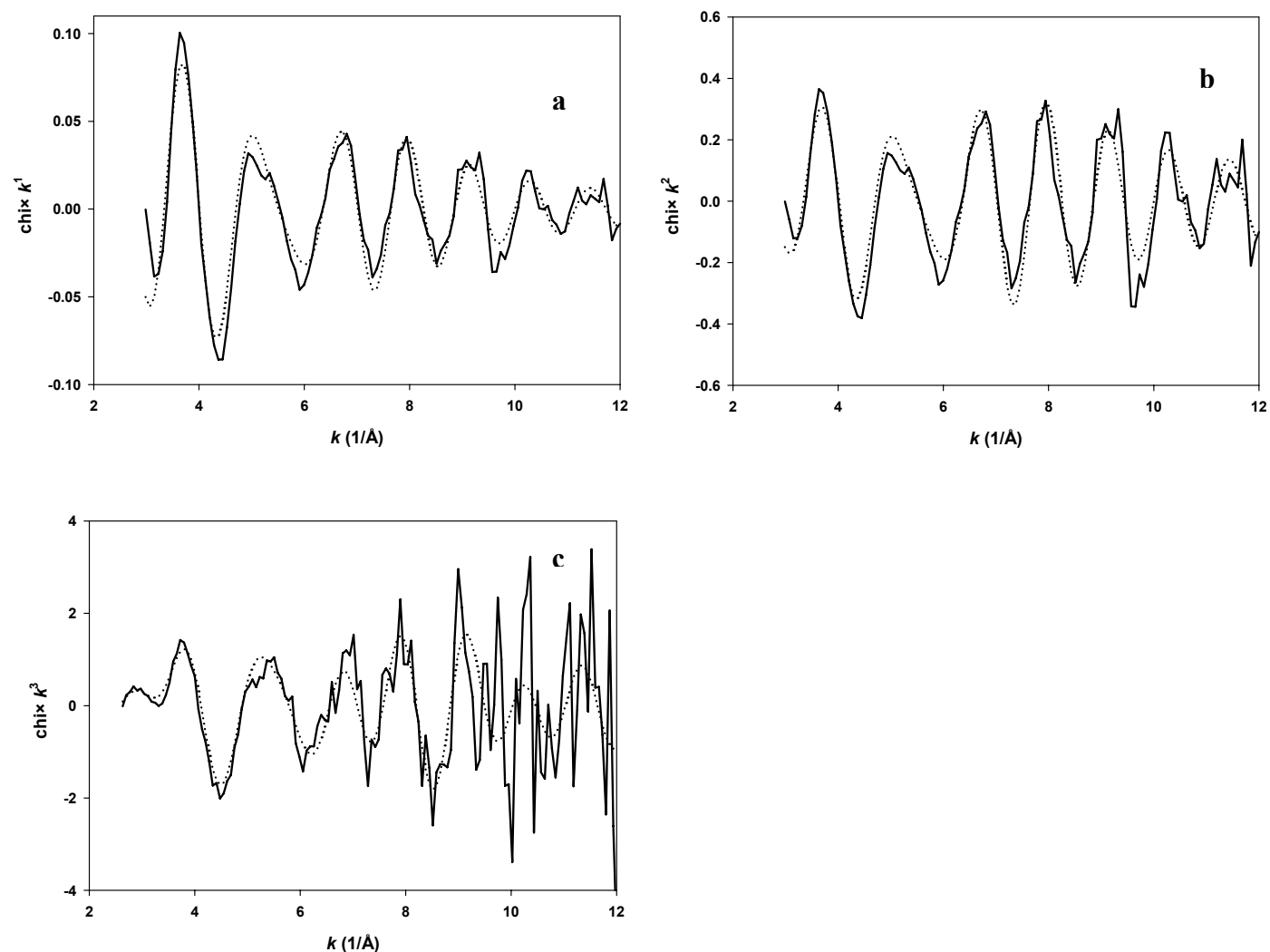


Fig. SI14. Experimental EXAFS function (solid line) and sum of the calculated contributions (dotted line) characterizing the sample after 48 h under CO oxidation reaction conditions at 353 K. (a) k^1 -weighted, (b) k^2 -weighted, and (c) k^3 -weighted. The k^3 -weighting emphasizes the data obtained at high values of k .

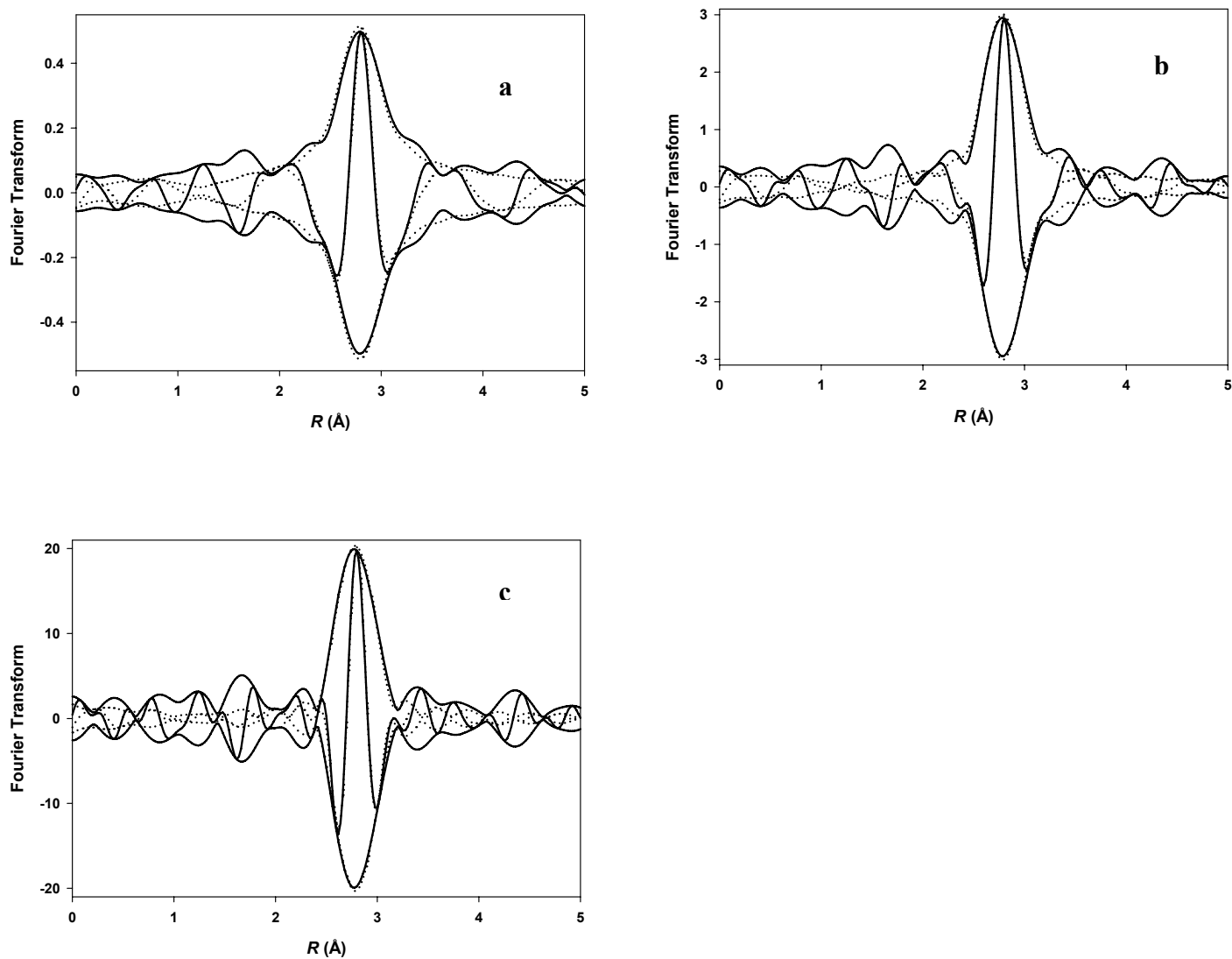


Fig. SI15. Imaginary part and magnitude of corrected Fourier transform of experimental EXAFS function (solid line) and the calculated Au—Au contribution (dotted line) characterizing the sample after 48 h under CO oxidation reaction conditions at 353 K. (a) k^1 -weighted, (b) k^2 -weighted, and (c) k^3 -weighted.

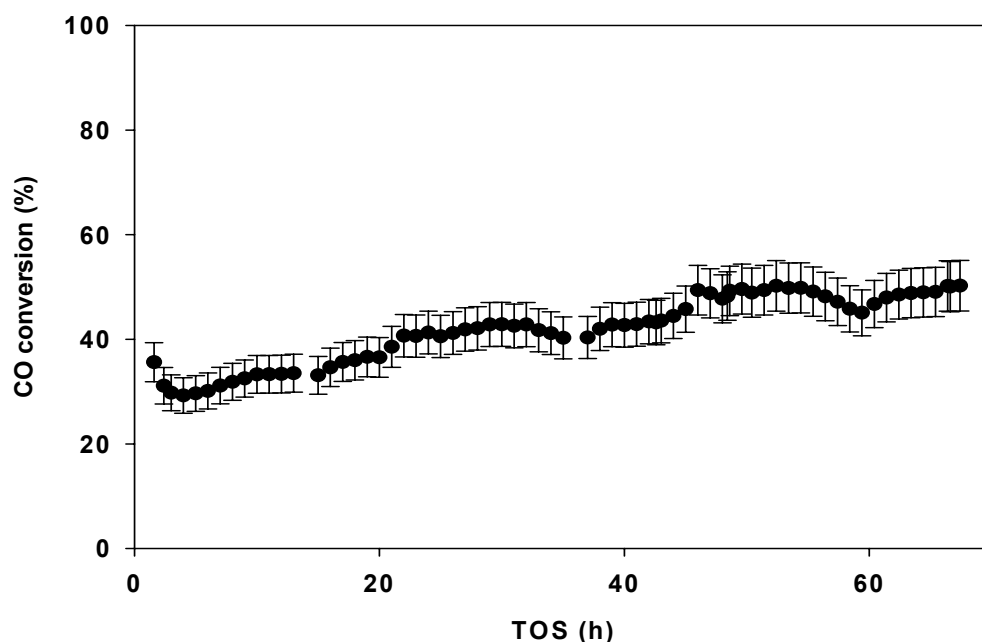


Figure S116a. Catalytic activity of gold supported on CeO_2 for CO oxidation at 298 K, after activation by operation as a catalyst for 50 h in a flow reactor at 353 K. Reaction conditions are stated in the text.

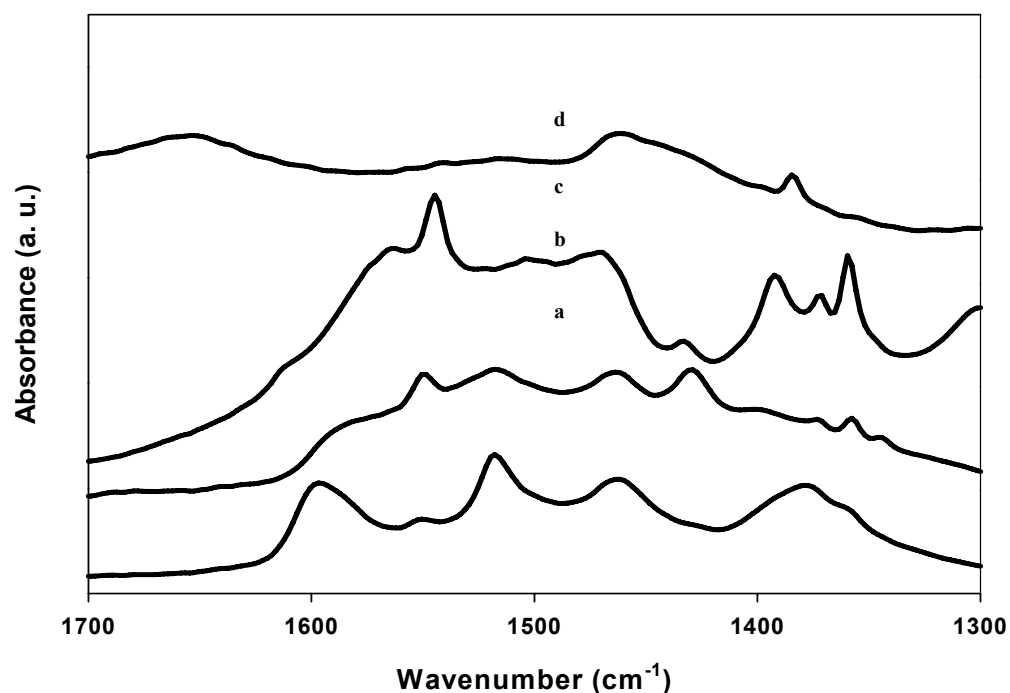


Figure S116b. IR spectra of gold supported on CeO_2 showing the removal of the acac ligands as the sample was used as a catalyst: (a) as-prepared sample, (b) sample after 2 h in flowing He [100 mL(NTP)/min] at 353 K, (c) after 2 h of operation as a CO oxidation catalyst at 353 K, and (d) after 24 h of operation as a CO oxidation catalyst at 353 K.

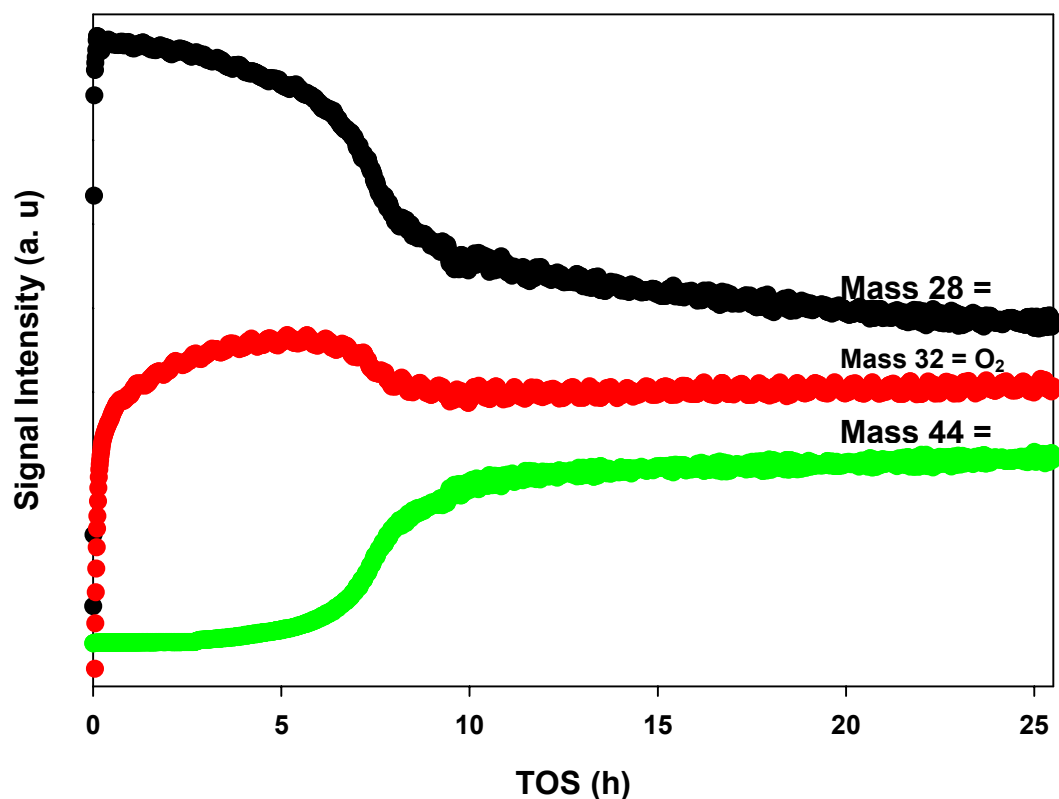


Figure SI17. Mass spectra of products of catalysis of CO oxidation at 353 K and 1 bar. Partial pressures of CO and O₂ were 10.1 and 5.7 mbar, respectively.

REFERENCES

1. D. C. Koningsberger, B. L. Mojet, G. E. Dorsen and D. E. Ramaker, *Top. Catal.* 2000, **10**, 143.
2. E. A. Stern, *Phys. Rev. B*, 1993, **48**, 9825.
3. J. C. Fierro-Gonzalez, V.A. Bhirud and B. C. Gates, *Chem. Commun.*, 2005, 5275.
4. S. Carrettin, P. Concepción, A. Corma, J. M. López Nieto and V. F. Puntes, *Angew. Chem. Int. Ed.*, 2004, **43**, 2538.
5. J. C. Fierro-Gonzalez and B. C. Gates, *J. Phys. Chem B*, 2004, **108**, 16999.
6. C. K. Costello, M.C. Kung, H.-S. Oh, Y. Wang, and H.H. Kung, *Appl. Catal. A* 2002, **232**, 159.
7. N. A. Hodge, C. J. Kiely, R. Whyman, M. R. H. Siddiqui, G. J. Hutchings, Q. A. Pankhurst, F. E. Wagner, R. Rajaram and S. Golunski, *Catal. Today*, 2002, **72**, 133.
8. G. J. Hutchings, M. S. Hall, A. F. Carley, P. Landon, B. E. Solsana, C. J. Kiely, A. Herzing, M. Makkee, J. A. Moulijn, A. Overweg, J. C. Fierro-Gonzalez, J. Guzman and B. C. Gates, *J. Catal.*, 2006, **242**, 71.
9. G. R. Bamwenda, S. Subota, T. Nakamura and M. Haruta, *Catal. Lett.*, 1997, **44**, 83.